Improved $d+{}^4$He potentials by inversion: The tensor force and validity of the double folding model

V. I. Kukulin and V. N. Pomerantsev
Institute of Nuclear Physics, Moscow State University, Moscow 119899, Russia

S. G. Cooper
Physics Department, The Open University, Milton Keynes, MK7 6AA, United Kingdom

S. B. Dubovichenko
Department of Physics, Kazakh State National University, Almaty 480121, Kazakhstan
(Received 17 November 1997)

Improved potential solutions are presented for the inverse scattering problem for $d+{}^4$He data. The input for the inversions includes both the data of recent phase shift analyses and phase shifts from RGM coupled-channel calculations based on the *NN* Minnesota force. The combined calculations provide a more reliable estimate of the odd-even splitting of the potentials than previously found, suggesting a rather moderate role for this splitting in deuteron-nucleus scattering generally. The approximate parity-independence of the deuteron optical potentials is shown to arise from the nontrivial interference between antisymmetrization and channel coupling to the deuteron breakup channels. A further comparison of the empirical potentials established here and the double folding potential derived from the M3Y effective *NN* force (with the appropriate normalization factor) reveals strong similarities. This result supports the application of the double folding model, combined with a small Majorana component, to the description even of such a loosely bound projectile as the deuteron. In turn, support is given for the application of iterative-perturbative inversion in combination with the double folding model to study fine details of the nucleus-nucleus potential. A d-^{4}He tensor potential is also derived to reproduce correctly the negative ^{6}Li quadrupole moment and the D-state asymptotic constant. [S0556-2813(98)03905-3]

PACS number(s): 25.45.De, 21.30.Fe, 24.10.−i, 21.60.Gx

I. INTRODUCTION

Many basic features of the interactions between light composite particles are now well established. In particular, a good description [1–6] of the interactions of light nuclei such as $d+t$, $t+{}^3$He, ^{4}He$+{}^4$He, etc. is obtained from a deep attractive potential with Pauli-forbidden states with the addition of parity dependence, Young scheme splitting, and a spin-orbit interaction. Importantly, this type of interaction is now justified from microscopic considerations, both in the quasiclassical picture [4] and also in the quantum mechanical shell-model framework [1,7]. These results lead to a general comprehensive understanding of the interrelations between various interaction models which appear, at first glance, to contradict each other.

Nevertheless, a number of finer features of the interaction, notably the role of the dynamic polarization of loosely bound projectiles such as d or ^{6,7}Li when combined with antisymmetrization effects, are not yet fully understood despite many previous efforts. The existing problems and contradictions are illustrated by the following example. On the one hand, it is well known (see, e.g., [1,8–13]) that antisymmetrization and coupled-channel effects in composite particle scattering unavoidably result in complex nonlocal and energy-dependent potentials, in which the breakup channels (with their various angular momenta in the relative motion of the fragments) lead to rather peculiar contributions in r space and the specific energy dependence. On the other hand, for a long time it has been standard practice to describe the elastic scattering of deuterons and nuclei such as ^{6}Li by the standard optical model (via local potentials) with a smooth energy dependence, or even by global optical models [14].

The low energy $N+{}^4$He interaction presents a further example of these problems. An attempt undertaken long ago by Satchler *et al.* [15], to describe $N+{}^4$He phase shifts for $E_N<20$ MeV by a standard optical potential of Woods-Saxon form, required a significant energy dependence in the *radial form* of the potential (i.e., of geometric parameters). Further studies based on S matrix to potential inversion [16,17], showed that the $N+{}^4$He phase shifts can be described excellently over a wide energy range ($E_N<65$ MeV) with a Gaussian-like potential with odd-even splitting and with a small energy dependence in the potential depth alone. This odd-even splitting is a direct consequence of antisymmetrization [1,5,18]. Thus the artificial energy dependence found by Satchler *et al.* [15] reflects only the omission of the odd-even splitting in the $N+{}^4$He potential.

Similar problems are also expected to arise for $d+{}^4$He and analogous systems. Moreover, many previous studies of deuteron scattering have demonstrated [12,13,19] the strong contribution of deuteron breakup channels, in particular with $\Delta l=2$, i.e., through the excitation of the D state in the N-N subsystem.

We can then ask, in what way can the above strong nonlocal contribution be incorporated into, say, the double folding potential, which, at first glance, contains no such effects? (Here we must emphasize that the usual type of nonlocalities

considered in the literature [9,10] differs from the terms, singular in energy, arising when the virtual breakup channels are excluded.) The important problem which must then be solved is to formulate the above nonlocal and specific energy dependent effects in terms of an ''exact'' optical potential, i.e., one which is reconstructed by inversion from the data or from microscopic theory as opposed to a standard phenomenological optical potential with a prescribed form (and fitted parameters).

Our plan of study is as follows. As a first approach, iterative perturbative (IP) inversions are presented based on phase-shift analyses of experimental data. These inversions follow Ref. [16], in directly calculating an explicit Majorana exchange force, instead of applying separate inversions for even and odd partial amplitudes as in previous determinations of the empirical $d+\alpha$ potential [20]. In this way the even and odd partial amplitudes are treated simultaneously and the inversion process is considerably stabilized. In the second approach, an extended RGM study is presented for the same system in order to gain a deeper understanding of the complicated interplay between antisymmetrization and projectile breakup effects. Increasing the number of coupled channels in these RGM calculations leads to three sets of microscopic models for the d-^{4}He interaction: (i) the direct d-^{4}He potential without incorporation of any exchange effects and which is related to standard double folding (df) models (see, e.g., [21]), (ii) the one channel ($d+^4$He) RGM model with full antisymmetrization but with a ''frozen'' deuteron, and (iii) the multichannel RGM model inclusive of breakup channels. RGM potentials are determined by inversion from the phase shifts of the last two models. The comparison of these different potential models then yields the contributions of antisymmetrization and deuteron breakup effects in terms of the local potential. The further comparison of our new empirical parity dependent solutions and the RGM solutions allows *quantitative* deductions to be made on the validity of the df model for the deuteron projectile (as applied in [24] for example). Our approach has one further advantage, since the considerable flexibility of the inversion method allows the determination of potentials, which describe the system under study not at a single energy but for a wide energy range simultaneously (previously denoted as ''mixed case'' inversion [17,22,23]).

The final part of our study is dedicated to a reconstruction of the tensor part of the d-^{4}He interaction. Here we study the range and depth of the d-^{4}He tensor force and compare it with the same quantities for central and spin-orbital components of the same system.

The contents of this work are then as follows. In Sec. II we describe, in brief, our inversion method and discuss the importance of including odd and even partial waves simultaneously in the inversion. Section IV describes the empirical input data used and presents a new solution for the empirical case. Section V is devoted to inversion of RGM calculations for $d+^4$He, which include coupling to the virtual breakup channels. Section VI contains a detailed discussion of the validity of the df model. In Sec. VII, we describe the calculation of a tensor d-^{4}He potential which nicely fits the ^{6}Li quadrupole moment and the tensor mixing parameter ε_1. Our findings are summarized in a concluding section.

II. THE INVERSION METHOD

The inversion method used in the next sections has been developed in Moscow (in the Moscow State University) [20,22,23,25] and independently in the Open University by Mackintosh and co-workers (originally in Ref. [26], with further developments and references in Ref. [16]). It has been named as the iterative-perturbative (IP) method by the latter group and as the linearized iterative method by the Moscow group. The two approaches have only minor differences which relate to the choice of inversion basis and details of the iteration process. The overall method is extremely flexible and convenient to use. It enables us to reconstruct many types of potentials, central, spin-orbit and tensor, real and complex, both from phase shifts or directly from scattering observables. The appropriate input quantities, e.g., S matrix, differential cross sections, analyzing powers etc. are nonlinear functions of the interaction potential and so may be considered as a functional response to variations in the interaction potential. In general, excluding some special cases, a small variation of the interaction potential is directly related to a small variation of the S matrix or other response function.

The basic idea behind the approach is then a local linearization of the response function in neighborhood of a given point in an appropriate functional space. This local linear approximation, together with an expansion of the unknown potential in some complete basis (for example the Fourier expansion in an orthogonal basis [20,22,23,25] or Gaussian functions that worked well in inversions for $p+\alpha$ [16]), results in a set of linear algebraic equations to be solved to yield the expansion coefficients. The initial approximation (i.e., initial values of the expansion coefficients or a starting reference potential) is usually chosen based on physical considerations. In particular, as will be shown in later sections, the results of the present paper suggest that a good choice for the initial potential would be the df potential. This initial potential is then corrected with step-by-step iterations which converge rapidly (5–7 iterations at most are usually required). A stable solution results for the first expansion coefficients of the sought potential and the number of reconstructed coefficients depends directly on the completeness and consistency of the input data.

The approach developed by the Moscow group has also been successfully applied [27] to reconstruct interactions in the field of heavy ion scattering in systems such as ^{12}C+^{13}C, ^{16}O+^{17}O, etc. The algorithm developed at the Open University has also been applied to a wide range of systems; for example to $p+^{16}$O directly from experimental observables [28], to mixed case N-nucleus phase shifts calculated from nonlocal interactions [29], and to single energy empirical S matrices, for nuclei such as ^{16}O+^{16}O [30], and for ^{11}Li scattering [31].

III. PARITY DEPENDENCE IN INVERSION

The general form of operator (or potential) of particle interaction can be expressed as follows:

$$V = V_W + \hat{M} V_M \tag{1}$$

where V_W is the Wigner-type interaction which includes the central, spin-orbit, and tensor interaction terms, i.e.,

$$V_W = V_W^{(c)} + V_W^{(sl)}\mathbf{l}\cdot\mathbf{s} + V_W^{(t)}\hat{S}_{12}, \tag{2}$$

V_M is the Majorana type interaction which includes, in general, similar terms, i.e., central, spin-orbit, and tensor, and $\hat{M}$ is the Majorana exchange operator. In the case here, for the interaction of two nuclei, a and b, $\hat{M} = P_{ab} = (-1)^{l_{ab}}$ and l_{ab} is a relative angular momentum of the pair a and b. Furthermore, in the standard approach the operator (1) can be rewritten in the form

$$\begin{aligned} V &= (V_W^{(c)} + P_{ab}V_M^{(c)}) + (V_W^{(ls)} + P_{ab}V_M^{(ls)})\mathbf{l}\cdot\mathbf{s} \\ &\quad + (V_W^{(t)} + P_{ab}V_M^{(t)})\hat{S}_{12} \\ &= \sum_{k=c,ls,t} (V_W^{(k)} \pm V_M^{(k)})A^{(k)} \end{aligned} \tag{3}$$

where the operators

$$A^{(k)} = \begin{cases} 1, & k=c, \\ \mathbf{l}\cdot\mathbf{s}, & k=ls, \\ \hat{S}_{12}, & k=t,^1 \end{cases} \tag{4}$$

and the plus sign relates to even partial waves and minus sign to odd partial waves. In this way, the interaction in the odd and even partial waves are uncoupled and each one can be parametrized and determined *independently* from the other.[2]

The procedure by which two inversions are applied to establish the odd and even components of interaction potentials independently will be denoted here as ''*separate*'' inversion. This method has been previously applied to $p+{}^4$He [17] and $d+{}^4$He [20,25].

The presence of well-expressed low-energy $d+{}^4$He resonances in the $L=2$ partial waves and near the S-matrix pole in the S wave has been shown previously [20,23,25] to render the solution of the inverse problem for the above channels so reliable that the data for even a small energy interval 0–5 MeV is sufficient to give quite a correct reconstruction of d-^{4}He interaction potential in even partial waves. In sharp contrast to this, the odd partial amplitudes are derived from the phase shift analysis with large errors due to a low sensitivity of majority of observables (cross sections and tensor analyzing powers) to these odd-parity partial phase shifts. As a result, the odd parity solution of the inversion has large errors which become more enhanced at the higher energies [20,25]. Hence, when the odd and even partial amplitudes are treated *independently* in the inversion [20,23,25], the magnitude and radial form of the Majorana interaction term cannot be established with sufficient accuracy. However, the structure of this term is very important for our understanding of the role and significance of exchange effects in nucleus-nucleus interactions.

The alternative approach is to derive the odd and even potential components simultaneously using the original form of interaction operator (3), i.e., to be denoted ''*simultaneous*'' inversion, as first introduced in Ref. [16]. For the inversion of $p+{}^4$He empirical phase shifts the two approaches lead to very similar potentials. However, simultaneous inversion was necessary to provide a stable parity-dependent inversion of $p+{}^{16}$O scattering observables [28], because the Majorana term is very small in comparison to the Wigner-type interaction. On the same note, it is common practice to apply inversion to whole multiplet of partial amplitudes, $\vec{J} = \vec{L} + \vec{1}$, simultaneously, i.e., to determine central and spin-orbit potentials directly rather than to calculate potentials for the separate spin channels with $J = L-S, \ldots, L+S$.

The general philosophy behind the simultaneous approach is the following. While the Majorana components describe exchange terms in the nucleus-nucleus interaction [5,12], these components represent only a minor part of the exchange correction compared to that contributing to the main Wigner term, the term which appears in the conventional simple and double folding models. This difference suggests that a more stabilized inversion is obtained by expanding V_W and V_M in separate basis sets, as in Ref. [28], i.e.,

$$V_W(r) = \sum_{i=0}^{N_1} C_i^{(1)}\phi_i^{(1)}(r), \tag{5}$$

$$V_M(r) = \sum_{j=0}^{N_2} C_j^{(2)}\phi_j^{(2)}(r). \tag{6}$$

Here $\phi^{(1)}$ and $\phi_j^{(2)}$ are basis sets with appropriate, but possibly differing radial scale parameters.

This approach then leads to a more reliable determination of the radial form and range of V_W and V_M compared to the potentials resulting from the separate inversion which may have significant uncertainties in the Majorana component. The inversions in the following section well illustrate the importance of simultaneous inversion. The two potential components are now simultaneously determined from even (well determined) and odd (poorly determined) partial amplitudes on equal footing. Applying a step-by-step extension of the basis in Eqs. (5) and (6) then yields a considerably stabilized inversion.

IV. STABILIZED INVERSION OF THE d-^{4}He EMPIRICAL DATA FOR $0 < E_d \leqslant 15$ MeV

A. The empirical $d+{}^4$He phase shifts

The inversions from empirical $d+{}^4$He data, described in the next section, are based on two separate sets of phase-shift analysis (PSA) data: (i) single energy PSA of the Zürich group [33] established for the energy range 6–43 MeV and (ii) the extended energy-dependent PSA of Kuznetsova *et al.* [34] for 0–10 MeV, with a special emphasis on the lowest energy region.

[1] In Sec. VII we use the standard S_{12} form for the tensor operator. A full classification for the tensor force based on symmetry principles was given by Satchler [10]. See also Robson [32].

[2] Formal mixing of odd and even partial waves is excluded due to parity conservation in nuclear interaction. Here we neglect a very small degree of mixing of the odd and even components due to the parity nonconserving terms.

As in previous inversions based in this PSA, tensor potential terms are excluded from all the inversion calculations presented here except those described in Sec. VII. The mixing parameter data are too poorly determined to give a stable inversion, due to the very weak influence of the tensor interaction on the low-energy phase-shifts, e.g., ε_1 differs from zero only in the narrow region near 6.5 MeV, where the $^3S_1$ and $^3D_1$ phase shifts are close in value. For similar reasons, only real potentials are determined due to the limitations in the inelasticity parameters. However, in Sec. VII we present a reconstruction of the ^{4}He$+d$ even-parity tensor potential from the ^{6}Li quadrupole moment and the existing PSA data for the ε_1 mixing parameter.

Although the PSA solutions of the Zürich group contain many irregularities and some nonmonotonic behavior, especially for $E_d>20$ MeV, the phase shifts in the energy range 6–14 MeV [33] are satisfactorily smooth functions of energy. On the other hand, the energy-dependent PSA [34] gives very reliable S- and D-wave phase shifts for $E_d<6$ MeV, which strongly stabilizes the inversion for both even and odd partial waves (see Sec. II). Therefore in this work we present results for inversions based on the phase shifts at energies up to 15 MeV only. A reconstruction of the d-^{4}He interaction using all the Zürich PSA data (up to 43 MeV), but by separate inversion, has been presented previously [20].

B. Inversion from the $d+^4$He phase shift analysis data

In this section we compare two solutions of the $d+^4$He inverse problem, determined using the algorithm developed by the Moscow group, for the energy range $0<E_d\leqslant 15$ MeV, obtained as follows: (i) by separate inversion of odd and even partial amplitudes [20], (ii) by simultaneous inversion of both amplitudes (present work). As a starting approximation we take only one term in the expansions of each potential component, e.g., central, spin-orbit, etc. Following our initial suggestions [22] we have used a s wave orthonormal harmonic oscillator basis, for which the first term of the series corresponds simply to a Gaussian. Then, in each subsequent stage, we add one term to each of the above components (either to each component alternately or to all components at once). If the input information is insufficient to determine the next expansion term, either the iterations fail to converge or the uncertainties in the expansion coefficients become too large, $\sim$100% [22]. The convergence of the method had been investigated previously [22,23] and here we only give the final results of the inversion.

In Figs. 1(a), 1(b) and 2(a), 2(b) we compare the potentials found for cases (i) and (ii) (the central components are displayed in Fig. 1 while the spin-orbit components are shown in Fig. 2).

The degree to which these two potentials reproduce the phase shifts is shown in Figs. 3 and 4 for the even and odd l-values, respectively. The apparent disagreement between the predictions of the inversion and the data of the phase shift analyses for the P waves (Fig. 4), probably arises due to the large errors in the PSA data for these amplitudes [33,34]. In particular, the results of accurate Faddeev calculations for d-^{4}He scattering [7,35] show a much better agreement with our predictions than with the PSA. So our simultaneous inversion for the P waves may be closer to the ''true'' solution than is apparent from Fig. 4.

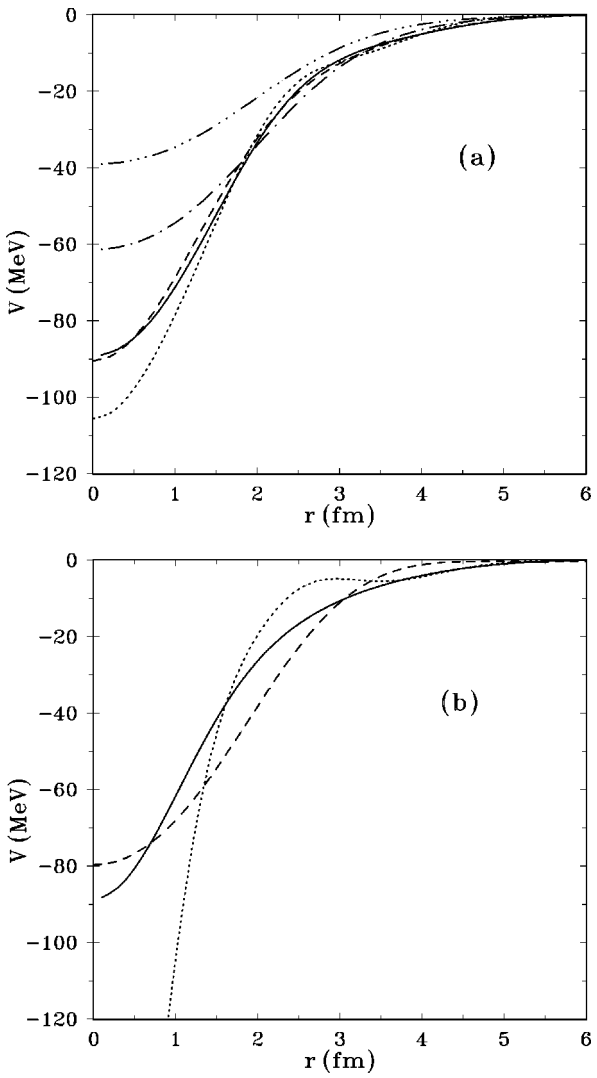

FIG. 1. (a) The central part of d-^{4}He potential for even partial waves reconstructed with PSA input data up to 15 MeV. The solid line is the result of simultaneous inversion (present work) and the dashed line represents the result of separate inversion [20]. Also shown is the potential obtained by separate inversion including energies up to 33 MeV [20] (dotted line), the df potential with the Minnesota NN force (triple dot-dashed line), and this df potential multiplied by $N_{\rm df}=1.572$ (dot-dashed line). (b) The central part of d-^{4}He potential for odd partial waves reconstructed with PSA input data up to 15 MeV. Solid line is the results of simultaneous inversion (present work), dashed line is from a separate inversion of odd-parity P and F waves [20], and the dotted line shows the inversion based on the P-wave phase shifts only.

It is evident from Figs. 1 and 2 that the modifications due to the improved stabilization of the inversion are comparatively small only for the even central potential. For the even spin-orbit and all the odd components, the differences are quite significant.

Strong changes are also found in the odd potential on inclusion of the F phase shifts in the input data [the dashed curve in Fig. 1(b)], when compared with inversion based on the P wave amplitudes alone [the dotted curve in Fig. 1(b)]. The solution based on P-wave phase shifts alone gives a

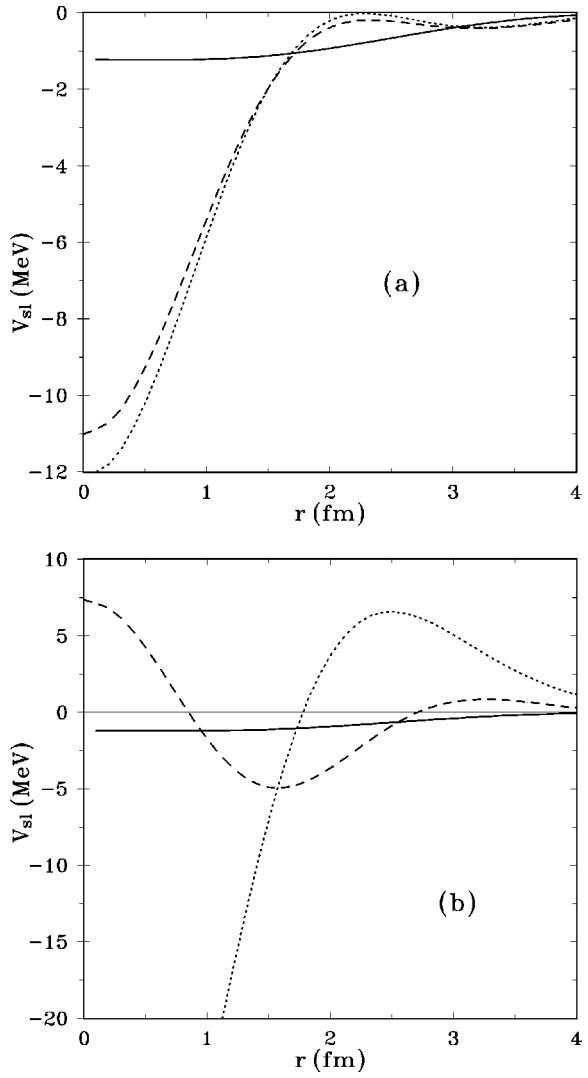

FIG. 2. (a) The d-^{4}He spin-orbit potential for even partial waves reconstructed with PSA input data up to 15 MeV. The notation is as in Fig. 1(a). (b) The d-^{4}He spin-orbit potential for odd partial waves reconstructed with PSA input data up to 15 MeV. The notation is as in Fig. 1(b).

very poor prediction of the F-wave phase shifts, even when taking into account the large errors in the F-wave phase shifts [33].

The above result is in agreement with our initial general expectation that incorporation even of rather ''noisy'' but *independent* input data into the inversion, together with some definite additional constraint (e.g., requiring some degree of smoothness in the potentials), leads to a noticeable stabilization of the solutions. This general feature of the IP inversion procedure then convincingly distinguishes our approach from more traditional and strict methods like Gel'fand-Levitan or Marchenko approaches. In the applications of the latter procedures, it is impossible to incorporate essentially incomplete or ''noisy'' data into the initial data set.

The forms for the Wigner and Majorana potentials are compared in Fig. 5. Clearly, the Wigner potential is peaked at the origin while the maximum of the Majorana potential is displaced to around 1.5 fm and its value is about 6 MeV, i.e., more than an order of magnitude less than the Wigner term. The relatively small value of the Majorana potential, which

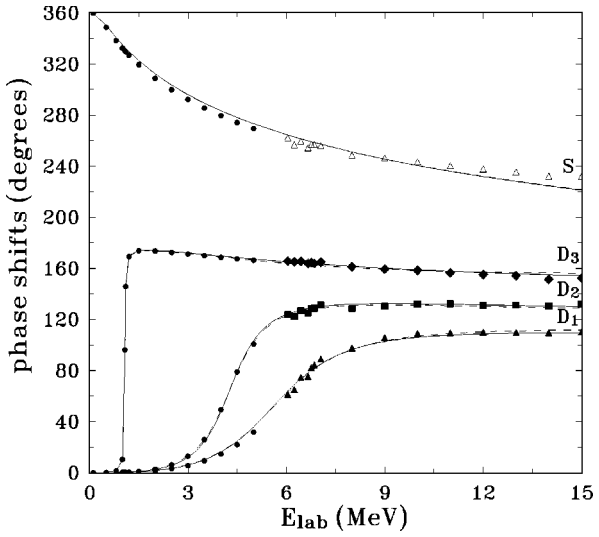

FIG. 3. The S- and D-wave phase shifts for the potential reconstructed by simultaneous inversion for energies up to 15 MeV (solid lines). Dashed lines show the results for inversion of even waves only [20]. PSA data are designated: ●–from [34], △, ▲, ■, ◆ from [33] for S and D_J waves ($J=L-1,L,L+1$), respectively.

arises as a manifestation of basic exchange effects, shows this contribution to be moderate in the present case. Microscopic multichannel RGM calculations presented in Sec. V confirm the relative difference in size of the Majorana and Wigner terms.

If a similar relation between Wigner and Majorana terms exists for the spin-orbit interaction as for the central components, there is no possibility of determining a Majorana (i.e., exchange) spin-orbit term from the existing PSA data. In fact, this supposition is confirmed by our results. The reasons for this are partly due to the errors in the PSA data as well as due to the small size of the Majorana spin-orbit term.

Thus, summarizing our findings in this section, we conclude that the effects of the odd-even splitting for $d+^4$He are rather moderate. This conclusion is also supported by the volume integrals,

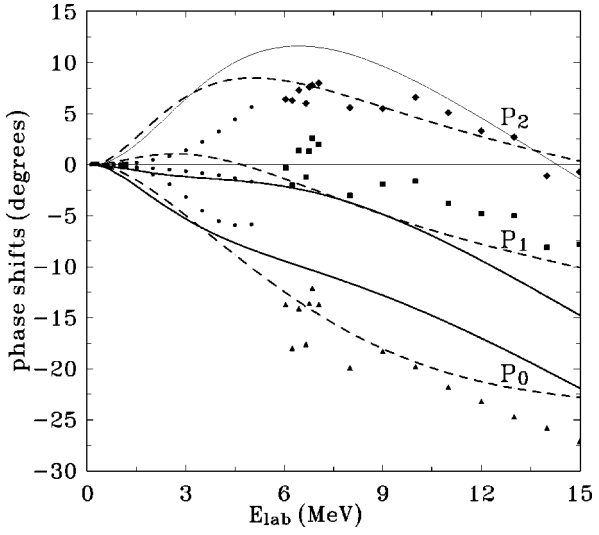

FIG. 4. Similar to Fig. 3 but for the P-wave phase shifts.

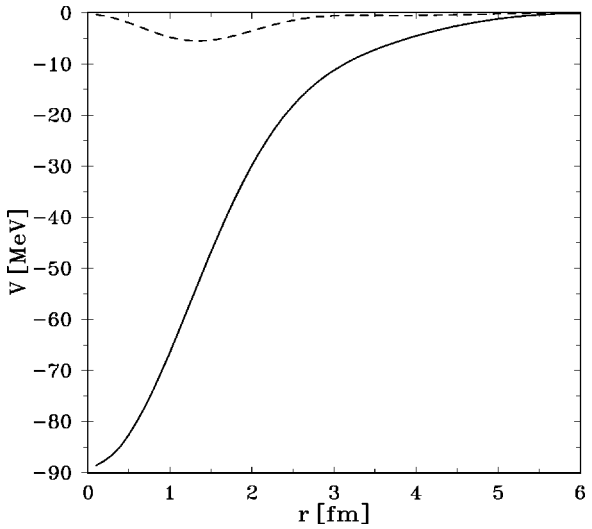

FIG. 5. Wigner V_W (solid line) and Majorana V_M (dashed line) parts of the central potential reconstructed from PSA input data up to 15 MeV.

$$J^{(k)} = -\frac{4\pi}{A_T A_P}\int V^{(k)}(r) r^2 dr \tag{7}$$

for the different components $V^{(k)}$ of the inverted potential, Eqs. (1)–(4). Table I displays the magnitudes of volume integrals $J^{(k)}$, for the potentials reported above.

We have also estimated the value of $J^{(c)}$ for the Majorana terms of the potentials determined by simultaneous inversion. These potentials give

$$J^{(c)}_{\text{even}} - J^{(c)}_{\text{odd}} = 2J^{(c)}_M \simeq 0.17 J^{(c)}_W ,$$

i.e., J_M is about 8.5% of J_W. Again, the Majorana term represents just a small correction to the main Wigner component.

The same interrelation between the Wigner and Majorana components should also be valid for the spin-orbit interaction and our stabilized inversion corroborates this conclusion. While the difference in volume integrals for the spin-orbit terms obtained from separate inversion of even and odd partial waves is quite remarkable (see Fig. 2), for simultaneous inversion this difference is beyond the accuracy achievable with the existing PSA. Thus we may conclude that the initial assumption on which the simultaneous inversion of even and odd parity states was based, i.e., that the interaction is of mainly Wigner type, is well justified by the results of the inversion.

TABLE I. Values of volume integrals $-(4\pi/8)\int V(r) r^2 dr$ [Mev fm^3] for different $d+^4$He potentials.

	Simultaneous inversion, present work	Separate inversion [20]	df with Minnesota force	df with DDM3Y [24]
Even waves	665.6	672.3	646.9	675.0
Odd waves	546.3	573.3		614.0
Spin-orbit	13.8	19.8		

V. INVERSION OF RGM $S(l)$ WITH BREAKUP CHANNEL CONTRIBUTIONS

The resonating group method (RGM) offers fundamental advantages for the study of the important effects contributing to $d+^4$He scattering, despite the simplified approximations necessary in the method. Here contributions to the potential due to both the full antisymmetrization of all nucleons and the inclusion of breakup channels can be directly assessed in a way not possible by inversion from empirical phase shifts. This formulation of the $d+^4$He RGM calculations closely follows the work of Kanada *et al.* [36], and the breakup channels are included using the pseudostate method described therein, although only $\Delta l = 0$ transfer is included.

The RGM S matrices are numerically calculated using modified forms of the codes of Blüge *et al.* [37], adapted to incorporate the Minnesota *NN* force [38] as described in a previous work [39]. The exchange mixture parameter $u = 0.97$, but the potentials described below are not sensitive to this value. The deuteron and excited n-p pseudostates are described by an 8 Gaussian basis [40], which allows coupling to 4 distortion channels of low energy deuteron excitation. No spin-orbit force is included in these calculations since the empirical spin-orbit terms cannot be determined to sufficient accuracy.

The RGM code yields tabulated S-matrix values which are input into the IP inversion code. As in Sec. IV, the inversion is confined to the energy range $0 < E_d < 15$ MeV. With the inclusion of channel coupling the S matrix becomes complex. At energies less than 10 MeV $|S|$ is close to unity, but at higher energies, the coupling to breakup channels produces an irregular variation of $|S|$ with energy. Other calculations show the imaginary potential arising from breakup coupling to have a marked variation with energy [20,41]. Since the imaginary potential cannot be established to any reliable accuracy over the energy range currently considered, all inversions in this section establish real potential components only.

The theoretical RGM phase shifts can be reproduced by inversion to a far greater accuracy than the empirical $S(l)$. However the most accurate inversions give irregularly shaped potentials due to an inherent, but small, energy dependence associated with the underlying nonlocality. This energy dependence of $S(l)$ cannot be reproduced by simply introducing an energy dependence in the potential magnitude, but requires a variation in the *potential form* with energy. Since the details of such a dependence are far beyond what can be determined empirically, only smooth energy independent solutions are now considered and these lead to an adequate fit to the phase shifts.

Solutions are obtained for both inversion methods described in Sec. II, i.e., for separate inversion of even and odd l-values and for simultaneous inversion to determine V_W and V_M. The choice of method is less critical in the case of theoretical $S(l)$ and, with a small inversion basis (two functions per component) the two methods lead to very similar parity dependent potentials. The simultaneous inversions also show that, using only a V_W term, a slightly more moderate fit to the RGM $S(l)$ results and thus the V_M component clearly represents only a small correction.

Figure 6 shows the even and odd l potentials for all four

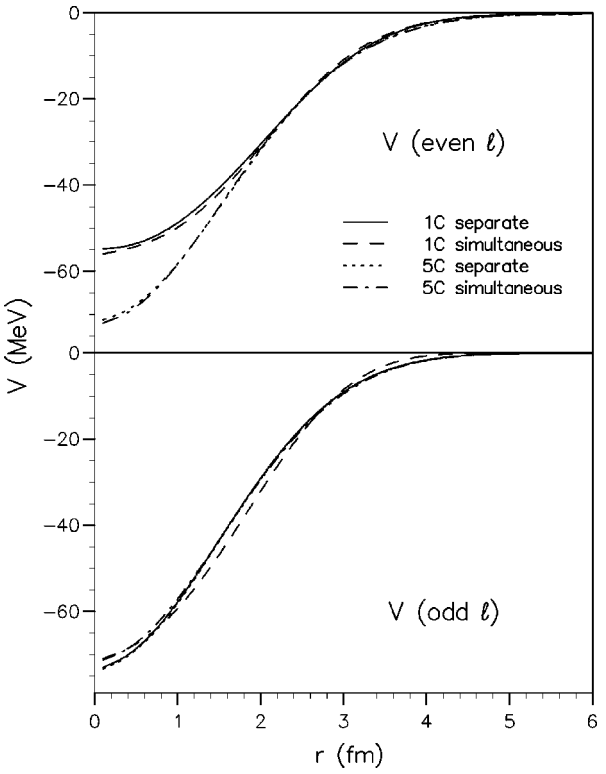

FIG. 6. Even (upper panel) and odd (lower panel) parity potentials determined from single channel RGM $S(l)$, by the two inversion approaches, separate (solid line) and simultaneous (dashed line), and from RGM $S(l)$ with breakup channel coupling by separate (dotted line) and simultaneous inversion (dot-dashed line).

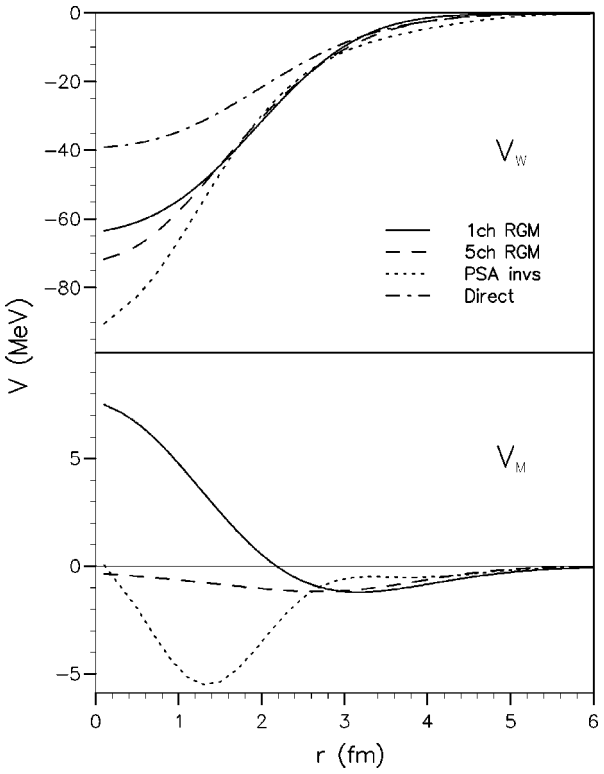

FIG. 7. The components V_W (upper panel) and V_M (lower panel) for simultaneous inversion from single channel RGM $S(l)$, (solid line) and from RGM $S(l)$ with breakup channel coupling (dashed line) compared with the empirical potential from simultaneous inversion (dotted line) and the RGM direct potential (dot-dashed line).

cases, i.e., with and without breakup coupling and using the two inversion approaches. The components V_W and V_M for the potentials obtained by simultaneous inversion are illustrated in Fig. 7 together with the RGM direct potential obtained from the double folding model for the Minnesota *NN* force. The breakup channels primarily change the even l phase shifts only [36], so that, although the even potential *increases* significantly in magnitude on inclusion of breakup coupling, there is little change in the odd component.

The restriction to energy-independent potentials leads to some uncertainties in the inversion but interesting results are revealed. The introduction of coupling produces both an increase in the Wigner potential magnitude at small radii and a small decrease at $r\sim 3$ fm. However, at larger radii the solution inclusive of breakup coupling is very close to the direct potential multiplied by $N_{\rm df}=1.572$ (see also Fig. 1).

The large changes in the even l phase shifts due to breakup coupling significantly decrease the parity dependence (i.e., the amplitude of the Majorana force) for $r<2$ fm. At larger radii there is a considerable agreement in the parity dependence for all solutions, but the strength of the V_M term barely exceeds 1 MeV.

The empirical solution presented in Sec. IV is indicated as the dotted line in Fig. 7. The limitations of the RGM calculations and its dependence on simple interactions, preclude the possibility of a very exact agreement with empirical results. Indeed the magnitude of V_M is too small at both larger radii and near the nuclear center, although the latter problem is improved by the addition of breakup coupling. Significantly, the inclusion of breakup effects brings the Majorana component closer to the empirical V_M potential, although the RGM potential is still too small in magnitude for $r<2$ fm. As a consequence, the net effective d-^{4}He RGM potential is close to a conventional *local* parity-independent potential. The empirical potential resulting from separate inversion has a much poorer agreement with the RGM solutions.

VI. VALIDITY OF DOUBLE FOLDING MODEL FOR d-^{4}He AND SIMILAR SYSTEMS

In the last two or three decades the df model has become extremely popular for the description of optical scattering, not only for p, ^{3}He(^{3}H), ^{4}He, etc., but also for such loosely bound particles as d, ^{6,7}Li or ^{9}Be [1,10,11,42–47]. However, for the latter projectiles the normalization constant $N_{\rm df}$ was found to deviate considerably from unity and is anomalously low. This problem has been explained [9,19,26,42,43], by the strong coupling effects of the virtual or real breakup of the loose projectile.

The accurate and fairly reliable potential for d-^{4}He established by inversion now allows us to study the behavior of the normalization constant in a more quantitative manner than was possible in the simple phenomenological analyses of deuteron scattering by medium and heavy nuclei [14].

The most important question here is how adequate is the df potential form? The general success of the df model apparently argues in favor of its correctness, but the situation here is far from trivial. The df potential (which corresponds to the so-called no-distortion approximation) must ad-

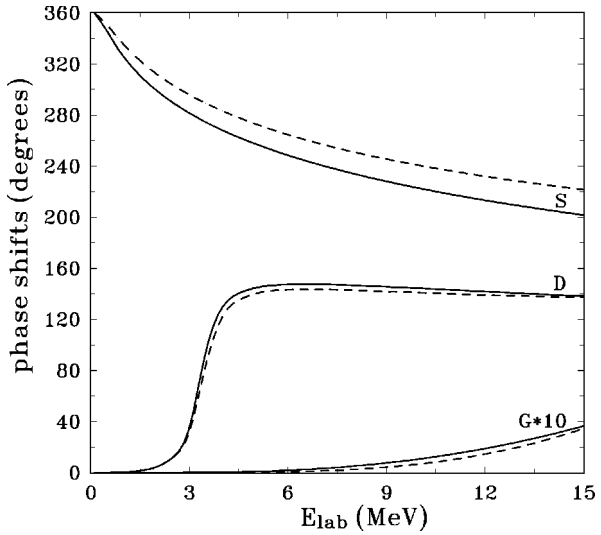

FIG. 8. Comparison between the *S*-, *D*-, and *G*-wave phase shifts for the double folding potential multiplied by $N_{\rm df}=1.572$ (solid lines) and the ''average'' phase shifts calculated with the central part of the reconstructed potential (dashed lines). (*G*-wave phase shifts are multiplied by 10 for convenience.)

equately describe only the peripheral part of the internuclear interaction where there is no distortion of the colliding nuclei. Moreover this is only achieved using an *NN* potential which has the correct peripheral behavior, and the normalization factor $N_{\rm df}$ should be close to unity. One then hopes that the short-range part of the internuclear interaction, where the effects of distortions and breakup are of greater importance, will be screened by a strong imaginary potential. In such circumstances the df model will be a good approximation for the exact interaction.

However, most practical applications of the df procedure are based on an effective *scalar NN* potential (usually the M3Y force) which is quite dissimilar to the true *NN* force. In such an approach the degree of similarity between the ''exact'' potential and the df potentials in both the peripheral and short-range radial regions is very interesting. Below we will try to answer these important questions.

In Fig. 1(a) a df potential, calculated with the effective *NN* Minnesota force, is compared with the stabilized solution of the inverse scattering problem described in Sec. II. It is evident that the *initial* df potential, even in the far peripheral region, is very different from the ''true'' interaction potential and the difference is rather large in the inner region.

Following standard practice [14], the df potential can be multiplied by a normalization coefficient, $N_{\rm df}$, and we find the even-parity partial amplitudes are most accurately reproduced with $N_{\rm df}=1.572$. The quality of fit to the phase shifts reached with this value of $N_{\rm df}$ is displayed in Fig. 8. Clearly the renormalized df potential provides a very reasonable fit to these phase shifts, with the exception of the *S* waves. In fact, the direct comparison of the renormalized df potential with potential obtained by inversion [see Fig. 1(a)] reveals that the peripheral parts ($r\geqslant 3$ fm) of both potentials are in reasonable agreement. In the inner region, however, there are large differences between the potentials which contribute significantly only to the *S*-wave phase shifts. The contributions of the short-range region will be further screened by the imaginary potential, which is present for $E_d>3.5$ MeV.

Further agreement is provided by a comparison of volume integrals, $J^{(k)}$, for the various potentials, as shown in Table I. In fact, the volume integral of the even parity potential, as determined by simultaneous inversion, is very close (with a difference of $\sim 1\%$ only) to that of the df potential [24], calculated with the standard (density-dependent) DDM3Y *NN* effective force and with $N_{\rm df}$ adjusted to reproduce the even l phase shifts. The equivalent comparison for the odd parity phase shifts shows far less agreement, and the volume integral of that M3Y df potential for odd l is closer to the volume integrals for the even parity cases. The volume integrals for the df potentials calculated with both the Minnesota and M3Y potentials (after multiplication by appropriate normalizing factors $N_{\rm df}$) are close to each other.

We can now turn to the role of deuteron breakup channels and antisymmetrization effects. The basic problem here, as was emphasized earlier, is how to reconcile the apparent contradiction between the rather good fit to scattering data given by the double folding model (with the M3Y force), on the one hand, although highly renormalized [10,11,43–46] and the proven contributions of the large effects of the virtual deuteron breakup channels [11–13]. In fitting the phase shifts with the df model only the *NN* effective force constant is adjusted, so that a good description of data means that the *radial form* of deuteron polarization potential[3] must be similar to the potential giving rise to purely elastic scattering, i.e., without any channel coupling. Thus the renormalized force constant in the df potential should effectively incorporate three important effects: (i) coupling with virtual breakup channels; (ii) antisymmetrization effects; and closely connected with the latter, (iii) the odd-even splitting effect.

Our conclusions derived in Sec. V of the present work and also in Refs. [12,13] can be summarized as follows:

(1) The Majorana force component, although definitely contributing, plays a rather moderate ($\sim 8\%$) role and hence does not destroy the good quality of fit achieved with the pure central interaction potential of the df approach.

(2) Antisymmetrization and channel coupling effects are rather large when considered separately, but the effects compensate each other to a considerable degree.[4] Thus, the resulting net contribution is rather small (see Figs. 6 and 7).

The odd parity potential shows almost no change when the deuteron breakup channels are included, whereas the even potential changes, on average, by 15–25 % at small radii. The reason underlying this change is seen in Fig. 7 where one can see that both the Wigner term V_W and the Majorana term V_M deepen by ~ 10 MeV near the origin on inclusion of channel coupling. However, the interaction in the even partial waves is described by the combination $V_W(r)+V_M(r)$ while that for the odd partial waves is governed by the combination $V_W(r)-V_M(r)$. As a result, the

[3]We assume quite naturally that the excitation of tightly bound nucleus ^{4}He at $E_d\leqslant 15$ MeV can be safely ignored.

[4]This is quite clear from a physical point of view since inclusion of the deuteron breakup components with a large radial range leads to an effective stretching of the deuteron while the antisymmetrization with the compact α-cluster wave function acts in the opposite direction, i.e., produces a ''compressing'' effect on the deuteron.

channel coupling (CC) leads to a deepening of the even potential by ~20 MeV near origin and to almost no change in the odd potential component.

Moreover, as we have already observed, the net effect of CC is mostly short range (see the upper part of Fig. 6). In practice this short-range contribution is often screened by an imaginary potential and is effectively invisible. Contrary to this, the long-range contributions of CC, which originate particularly from real breakup effects, usually produce surface repulsion [19] and these contributions cannot be simulated by renormalizing the total *NN* force constant in fitting the $d+A$ scattering cross sections. However these surface repulsion terms are generally important only at higher energies $E_p \geqslant 20$ MeV and in our low-energy case they are unlikely to be important. In fact, the one-channel effective d-^{4}He RGM potential (see the solid and dashed curves on the upper part of Fig. 6), which takes into account only the antisymmetrization effects but not the coupling to breakup channels, is very similar to the renormalized df potential [see the dot-dashed curve on Fig. 1(a)].

The renormalized df potential then reproduces the ''true'' potential in the peripheral region ($r>2$ fm) quite well. However, the renormalized df potential is a little deeper than the ''true'' one in the intermediate region 2 fm $<r<$ 3 fm and also more shallow by ~20% than the true potential in the innermost region, $r<2$ fm. Consequently, when the df model is applied to deuteron scattering off light nuclei we expect to obtain quite a reasonable description of the elastic scattering cross section, but with some deviations from the data for the vector and especially the tensor analyzing powers, which are sensitive to variations of the odd l phase shifts and to interference effects.

A careful comparison of the potentials determined from RGM phase shifts calculated *without* channel coupling effects (solid lines in the upper part of Fig. 6) with the renormalized df potential $V_{\rm df}(r)$ [the dot-dashed line in Fig. 1(a)] shows that the deviation of the df potential from the true one is most likely to arise due to deuteron breakup channel coupling.[5] Therefore one expects the df model to give a highly accurate description when applied to the description of scattering of more dense and heavily polarized projectiles such as α particles. Recent work [45] confirms this conclusion.

Thus, the rather good agreement of both df and inversion potentials at intermediate and large distances, and in the phase shift behavior, does support the application of the df procedure for the description of deuteron scattering, even by the very light ^{4}He-nucleus.

VII. TENSOR d-^{4}He POTENTIAL AND THE ^{6}Li QUADRUPOLE MOMENT

The $d+^4$He tensor interaction has been neglected in the preceding sections due to the lack of reliable mixing parameters in the present PSA data. However, a tensor potential must be incorporated to describe the quadrupole moment of ^{6}Li nucleus.

TABLE II. Parameters of the tensor potential for $d+^4$He.

Variant	V_0 [MeV]	α [fm^{-2}]	V_1 [MeV]	β [fm^{-2}]
A	−71.979	0.20	27.0	1.12
B	−77.106	0.22	40.0	1.60

It is well known that the very small negative value of the ^{6}Li quadrupole moment ($Q=-0.0644$ fm^2) cannot be explained by the standard three-body $\alpha+2$N model [48], but probably originates through the coupling between the D-wave component of the α particle in the closed channel $d+d\rightarrow^4$He and the D-wave component of the $\alpha+d$ relative motion. The negative value of Q is associated directly with the negative value of the asymptotic mixing constant $\eta_D=-0.0125$ [49], i.e., the sign of the D component of the bound-state wave function (in the asymptotic region) must be *opposite* to that of the S component. A ^{6}Li wave function of this type has been formulated [47,48] and this model does give the correct sign of quadrupole moment.

Here we attempt to reconstruct a d-^{4}He potential which describes the $^3S_1$ and $^3D_1$ low-energy phase shifts and the main properties of the ^{6}Li ground state, including the quadrupole moment. Consequently the data input into the inversion includes the binding energy and quadrupole moment of ^{6}Li together with the phase shifts for energies up to 11 MeV. To retain stability in the inversion, we have restricted the expansions of both central and tensor parts of interactions to just one term:

$$V(r)=V_c(r)+V_t(r)S_{12}, \tag{8}$$

$$V_c(r)=-V_0\exp(-\alpha r^2) \tag{9}$$

$$V_t(r)=-V_1\exp(-\beta r^2). \tag{10}$$

Table II lists the parameters of two possible potentials satisfying the above criteria. The properties of the ^{6}Li ground state calculated from these potentials are presented in Table III, together with the corresponding experimental values. The $^3S_1$ and $^3D_1$ phase shifts and the mixing parameter ε_1, evaluated with the two potentials, are shown in Figs. 9 and 10 (solid lines are for variant A, dashed lines for variant B). The negative values of ε_1 can be obtained only from narrow tensor potentials. The use of wider potentials results

TABLE III. The properties of the ^{6}Li ground state, calculated with the reconstructed tensor $d+^4$He potential.

Properties	Potential A	Potential B	Experimental values
E_b [MeV]	−1.4735	1.4735	1.4735
R_r [fm]	2.60	2.56	2.56(5)
R_f [fm]	2.53	2.50	2.54(5)
Q [fm^2]	−0.064	−0.064	−0.0644(5)
C_0^0	1.9	1.9	2.15(10)
η_D	−0.0115	−0.0120	−0.0125(25)
μ_d/μ_0	0.848	0.847	0.822
P_D %	1.59	1.78	

[5]This conclusion is in agreement with the results of analysis of the scattering of other weakly bound projectiles like ^{6,7}Li, ^{9}Be, etc. [43,47].

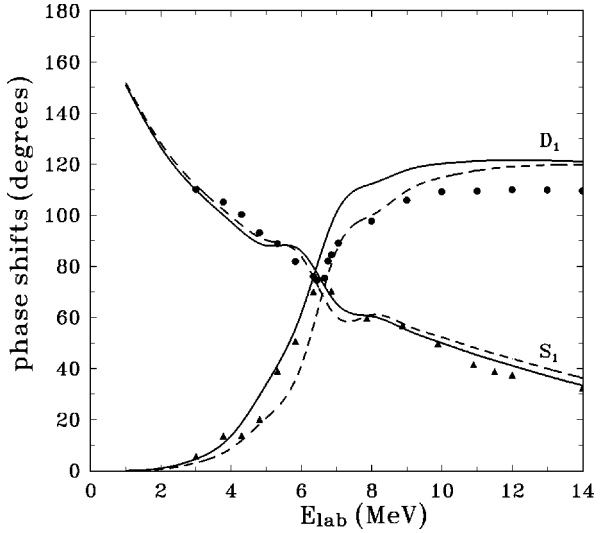

FIG. 9. The theoretical eigenphase shifts corresponding to the $^3S_1$ and $^3D_1$ phase shifts in the uncoupled channels and the PSA results. The circles and triangles display the PSA data. The solid and dashed lines correspond to the tensor potentials A and B, respectively.

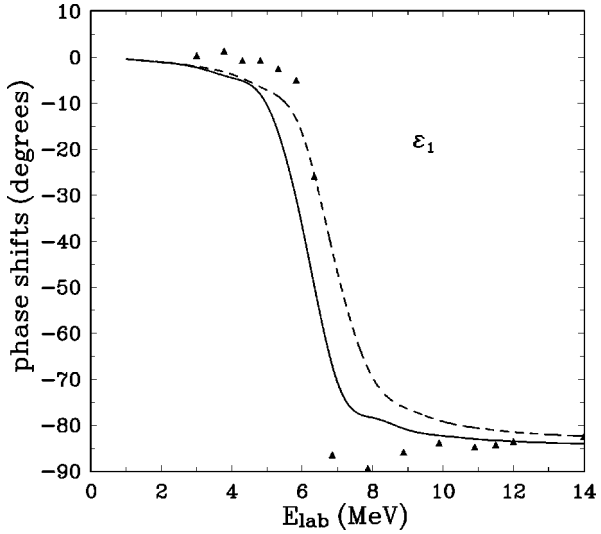

FIG. 10. The comparison between the theoretical and experimental values of the tensor mixing parameter ε_1. The solid and dashed lines correspond to the tensor potentials A and B, respectively.

in both a change of sign of ε_1 and a change of the asymptotic mixing constant of the ground state η_D. Thus the range of the d-^{4}He tensor potential is much less than that of the central potential. This finding provides evidence for a strong d-exchange contribution to the tensor d-^{4}He force [48][6] because the range of the exchange force in the exchange mechanism should be rather short due to the small rms radius of ^{4}He and the large binding energy in the channel $^4\text{He} \rightarrow d+d$.

A separate work is now in preparation to investigate further this short-range tensor force induced by the Pauli principle.

VIII. CONCLUSIONS

In this work we have studied some important problems relating to the interaction potential underlying the scattering of composite particles such as $d+^4$He. In order to establish the true interaction potential, we solved an inverse scattering problem using our effective method of linearized iterations. The input for the inversions include both phase shifts calculated from RGM coupled channel calculations, which incorporate virtual and real breakup channels, and the results of a recent phase shift analysis.

The success of the inversions presented here depended considerably on combining the very reliable even partial wave amplitudes with the ''noisy'' odd l values within the empirical data set. The Majorana exchange interaction was *explicitly* evaluated in the inversion, and by this procedure the odd parity potential is determined with greater stability. The resulting empirical potentials then represent an improvement on previous $d+^4$He potentials for which the odd parity potential was unreliable and inaccurate. The new stabilized empirical potential can be applied to predict improved phase shifts for the odd partial waves.

The new empirical potential agrees quite well with the RGM predictions for both the Wigner and the Majorana components of the potential, but only after inclusion in the RGM of the breakup channel coupling. The Majorana components of both the RGM and the empirical-phase-shift solutions are small in magnitude and this odd-even splitting is then expected to be of minor importance for other $d+A$ systems.

We have also compared these ''exact'' interaction potentials with the potentials calculated using the popular df model based on two different effective NN forces: (i) DDM3Y NN force, and (ii) Minnesota NN force. On whole the general agreement is reasonable for both effective forces. The DDM3Y force, multiplied by an appropriate normalization factor, leads to a better agreement with empirical potentials and provides a quite satisfactory reproduction of the ''experimental'' phase shifts (see also [14,24,44–46]). Nevertheless effects such as the odd-even splitting etc. are not included in the df approach.

This agreement of the df M3Y model with the empirical potential arises as a result of the interference of several effects omitted in the df model, notably antisymmetrization and breakup channels coupling. The RGM calculations show that the breakup effects only contribute noticeably to the even parity potential and have little effect on the odd parity component. These contributions of antisymmetrization and breakup coupling then mutually compensate each other in the peripheral nuclear region.

An analysis of $d+^{40}$Ca scattering at $E_d=52$ MeV [44], leads to very similar results, in particular in the interrelation between the df potential for $d+^{40}$Ca and the ''exact optical potential'' extracted from the data by a model independent analysis. Our findings may then have a much wider applicability than the particular case considered here.

Combining the above results leads to a very powerful in-

[6]This effect should be compared with the NN one-pion-exchange forces where both central and tensor components have the same range, μ^{-1} (μ is the pion mass).

version procedure. The modified IP inversion method, as employed widely in the present work, converges very fast and in a stable manner with a good choice of initial potential. We now suggest the df model as a convenient candidate for this initial approximation. The complete method, when invoked for inversion directly from cross-section data [25,28], offers many opportunities to study fine details of the interactions of complicated systems such as ^{24}Mg+^{112}Sn, ^{12}B+A, etc. and even for unstable radioactive projectiles scattered off stable targets (see, e.g., [50]).

In this paper we have also determined a d-^{4}He tensor interaction. The resulting potential is rather short ranged and is relatively large in amplitude ($\sim$30–40 MeV). As has been previously suggested [40], this interaction may arise due to the very specific exchange effect in which the ''inner'' deuteron in the D state of the ^{4}He core is exchanged with the outer valence deuteron. This exchange mechanism can explain both the short-range character of the d-^{4}He tensor force, through the very small rms radius of ^{4}He, and the *negative* value of the ^{6}Li quadrupole moment. The second result is consistent with the fact that the s-wave and d-wave components of the total ^{6}Li wave function, when projected onto the d-^{4}He channel, have opposite signs in the asymptotic region. Thus the form and strength of the d-^{4}He tensor force at both low and intermediate energies deserve detailed further study.

Many characteristic features of interaction of the d-^{4}He system have been established in this and a series of preceding works [1,7,20,23,25,34,40,48]. Important features such as the Pauli principle manifestation and the appearance of Pauli-forbidden states, the description of higher partial waves, channel coupling effects, the interrelation with supersymmetrical partner potentials and the general manifestation of dualism repulsion-attraction in composite particle interaction have now been studied in detail. In particular we have shown [1,3], that the deep attractive interaction potentials in the systems ^{4}He+^{4}He, ^{4}He+N, etc. arise as a consequence of well-localized Pauli-forbidden states and the appropriate conditions of orthogonality for the scattering wave functions to these forbidden states. In turn, the structure of the Pauli forbidden states is very closely interrelated to the shell model structure of the whole unified system [4,7]. Other interesting effects found concern the joint action of antisymmetrization and (virtual) breakup in $d+^4$He system [12]. These calculations establish that, while the inclusion of deuteron breakup channels *diminishes* the $d+^4$He cluster probability in the full three body ^{6}Li wave function, the subsequent antisymmetrization of the $n+p+^4$He wave function *increases* the $d+^4$He cluster probability. Again both these important contributions produce opposing effects. Thus the present paper can be considered, in some sense, as a very illuminating illustration of the fruitfulness of the six-nucleon system as a test study in nuclear physics.

ACKNOWLEDGMENTS

The authors are grateful to Professor V. Neudatchin, Dr. R. S. Mackintosh, and our colleagues at the Moscow Institute of Nuclear Research for useful discussions during the course of the work. The authors acknowledge financial support from the Engineering and Physical Sciences Research Council of the U.K. (under the grant GR/H00895) and from the Russian Foundation for Basic Research (grant 97-02-17265).

[1] V. I. Kukulin, V. G. Neudatchin, Yu. F. Smirnov, and I. T. Obukhovsky, *Clusters as Subsystems in Light Nuclei*, Vol. 3 in the series *Clustering Phenomena in Nuclei* (Vieweg & S. Verlag, Braunschweig/Wiesbaden, 1983).

[2] B. Buck, C. B. Dover, and J. P. Vary, Phys. Rev. C **11**, 1803 (1975); B. Buck and A. A. Pilt, Nucl. Phys. **A280**, 133 (1977).

[3] V. I. Kukulin, V. G. Neudatchin, A. A. Sakharuk, and V. N. Pomerantsev, Phys. Rev. C **45**, 1512 (1992); Yad. Fiz. **52**, 402 (1990); Phys. Lett. B **255**, 482 (1991).

[4] H. Horiuchi, Prog. Theor. Phys. **64**, 184 (1980).

[5] Y. C. Tang, M. LeMere, and D. R. Thomson, Phys. Rep. **47**, 167 (1978).

[6] S. G. Cooper, Phys. Rev. C **50**, 359 (1994).

[7] L. D. Blokhintsev, V. I. Kukulin, D. A. Savin, and A. A. Sakharuk, Yad. Fiz. **53**, 693 (1991).

[8] H. Feshbach, Ann. Phys. (N.Y.) **5**, 357 (1958).

[9] S. A. Sofianos, K. C. Panada, and P. E. Hodgson, J. Phys. G **19**, 1929 (1993).

[10] G. R. Satchler, *Direct Nuclear Reactions* (Clarendon Press, Oxford, 1983).

[11] T. K. Roy and S. Mukherjee, J. Phys. G **13**, 1239 (1987); G. H. Rawitscher, Phys. Rev. C **9**, 2210 (1974); Nucl. Phys. **A241**, 365 (1975).

[12] R. G. Lovas, A. T. Kruppa, R. Beck, and F. Dickman, Nucl. Phys. **A474**, 451 (1987); K. Varga and R. G. Lovas, Phys. Rev. C **43**, 1201 (1991); Y. Fujiwara and Y. C. Tang, *ibid.* **43**, 96 (1991); Few-Body Syst. **12**, 21 (1992): H. Kanada, T. Kaneko, and Y. C. Tang, Phys. Rev. C **38**, 2013 (1988).

[13] Y. Yahiro and M. Kamimura, Prog. Theor. Phys. **65**, 2046 (1981); **65**, 2051 (1981); V. I. Kukulin and V. N. Pomerantsev, Yad. Fiz. **50**, 27 (1989).

[14] J. Cook, Nucl. Phys. **A382**, 61 (1982).

[15] G. R. Satchler, L. W. Owen, A. J. Elwyn, G. L. Morgan, and R. L. Walter, Nucl. Phys. **A112**, 1 (1968).

[16] S. G. Cooper and R. S. Mackintosh, Phys. Rev. C **54**, 3133 (1996).

[17] S. G. Cooper and R. S. Mackintosh, Phys. Rev. C **43**, 1001 (1991).

[18] S. G. Cooper, R. S. Mackintosh, A. Csótó, and R. G. Lovas, Phys. Rev. C **50**, 1308 (1994).

[19] A. A. Ioannides and R. S. Mackintosh, Phys. Lett. **169B**, 113 (1986).

[20] V. I. Kukulin and V. N. Pomerantsev, Yad. Fiz. **60**, 1228 (1997).

[21] G. R. Satchler and W. G. Love, Phys. Rep. **55**, 183 (1979).

[22] V. I. Kukulin, V. N. Pomerantsev, and J. Horaček, Phys. Rev. A **42**, 2719 (1990).

[23] V. I. Kukulin and V. N. Pomerantsev, Yad. Fiz. **51**, 376 (1990).

[24] P. Mohr, V. Kölle, S. Wilmes, U. Atzrott, G. Staudt, J. W. Hammer, H. Krauss, and H. Oberhummer, Phys. Rev. C **50**, 1543 (1994); Z. Phys. A **349**, 339 (1994).
[25] V. I. Kukulin, V. N. Pomerantsev, and S. B. Zuev, Yad. Fiz. **59**, 428 (1996).
[26] R. S. Mackintosh and A. M. Kobos, Phys. Lett. **116B**, 95 (1982).
[27] A. Adahchour, D. Baye, and P. Descouvemont, Nucl. Phys. **A579**, 305 (1994).
[28] S. G. Cooper, Nucl. Phys. **A618**, 87 (1997).
[29] R. S. Mackintosh and S. G. Cooper, J. Phys. G **23**, 565 (1997).
[30] S. G. Cooper and R. S. Mackintosh, Nucl. Phys. **A576**, 308 (1994).
[31] S. G. Cooper and R. S. Mackintosh, Nucl. Phys. **A582**, 283 (1995).
[32] B. A. Robson, *The Theory of Polarization Phenomena* (Clarendon Press, Oxford, 1974).
[33] B. Jenny, W. Grüebler, V. König, P. A. Schmelzbach, and C. Schweizer, Nucl. Phys. **A397**, 61 (1983).
[34] E. V. Kuznetsova and V. I. Kukulin, Yad. Fiz. **60**, 528 (1997); V. M. Krasnopol'sky, V. I. Kukulin, E. V. Kuznetsova, J. Horaček, and N. M. Queen, Phys. Rev. C **43**, 822 (1991).
[35] Y. Koike, Prog. Theor. Phys. **59**, 87 (1978).
[36] H. Kanada, T. Kaneko, S. Saito, and Y. C. Tang, Nucl. Phys. **A444**, 209 (1985).
[37] G. Blüge, K. Langanke, and H.-G. Reusch, in *Computational Nuclear Physics 2*, edited by K. Langanke, J. A. Maruhn, and S. E. Koonin (Springer-Verlag, New York, 1993).
[38] D. R. Thompson, M. LeMere, and Y. C. Tang, Nucl. Phys. **A286**, 53 (1977).
[39] S. G. Cooper, Nucl. Phys. **A626**, 715 (1997).
[40] V. I. Kukulin and G. G. Ryzhikh, Prog. Part. Nucl. Phys. **34**, 397 (1995).
[41] R. S. Mackintosh and S. G. Cooper, Nucl. Phys. **A625**, 651 (1997).
[42] M. Kamal, V. T. Voronchev, and V. I. Kukulin, Vopr. At. Nauki Tekh., Ser.: Yad Konstanty **4**, 42 (1989); J. Phys. G **18**, 379 (1992).
[43] C. Samanta, S. Ghosh, M. Lahiri, S. Ray, and S. R. Banerjee, Phys. Rev. C **45**, 1757 (1992); T. Sinha, S. Ray, and C. Samanta, *ibid.* **48**, 785 (1993).
[44] M. Ermer, H. Clement, P. Grabmayr, G. J. Wagner, L. Friedrich, and E. Huttel, Phys. Lett. B **188**, 17 (1987).
[45] U. Atzrott, P. Mohr, H. Abele, C. Hillenmayer, and G. Staudt, Phys. Rev. C **53**, 1336 (1996).
[46] H. Abele and G. Staudt, Phys. Rev. C **47**, 742 (1993).
[47] N. Nishioka, J. A. Tostevin, R. C. Johnson, and K. I. Kubo, Nucl. Phys. **A415**, 230 (1994).
[48] V. I. Kukulin, V. N. Pomerantsev, Kh.D. Razikov, V. T. Voronchev, and G. G. Ryzhikh, Nucl. Phys. **A586**, 151 (1995).
[49] H. R. Weller and D. R. Lehman, Annu. Rev. Nucl. Part. Sci. **38**, 563 (1988); R. Crespo, A. M. Eiro, and F. D. Santos, Phys. Rev. C **39**, 305 (1989).
[50] S. A. Goncharov, A. S. Dem'yanova, and A. A. Ogloblin, ''Nucleon density distributions in ^{8}He and ^{8}B from elastic scattering by ^{3}He and ^{3}H,'' Moscow State University Preprint INP MSU 97-31/4482, 1997.